

Monitoring of Eyjafjallajökull Ash Layer Evolution over Payerne Switzerland with a Raman Lidar

T. Dinoev¹, V. Simeonov¹, B. Calpini², M. B. Parlange¹

¹ Environmental Fluid Mechanics Laboratory, Swiss Federal Institute of Technology; EPFL-ENAC-EFLUM, Station 2, CH1015 Lausanne, Switzerland; *tel*: +41 21 69 36 385; *fax*: +41 21 693 63 90; *e-mail*: valentin.simeonov@epfl.ch

² Payerne Aerological Station, MeteoSwiss; Les Invuardes, CH 1530 Payerne, Switzerland; *tel*: +41 26 662 62 28; *fax*: +41 26 662 62 12; *e-mail*: bertrand.calpini@meteoswiss.ch

Abstract

The ash layer from the erupted volcano Eyjafjallajökull in Iceland was monitored with the continuously operated MeteoSwiss/EPFL Raman lidar installed at the MeteoSwiss aerological station in Payerne. Aerosol scattering ratio profiles were measured allowing observations of the vertical extent and time evolution of the layer. Ash density profiles were calculated as well using preliminary ash density estimation from an in-situ measurement. These measurements demonstrated the ability of ground based lidars to monitor the vertical distribution of ash layers providing valuable information to the aviation authorities.

1. Introduction

The Iceland volcano Eyjafjallajökull started to emit significant amount of volcanic ash on 15 April 2010 following the initial eruption on 20 March 2010. In the next days, the ash layer was dispersed over most parts of Europe. Since the glassy particles in the volcanic ash are potentially dangerous for the airplanes, the European airspace, except for some Southern parts, was closed for several days.

In order to define the conditions at which the airspace could be open, quantitative information about spatial and temporal evolution of the layer was urgently needed. Satellite, airborne and ground observations together with meteorological models were used to evaluate the evolution of the layer. While the horizontal extent of the ash layer was accurately captured by satellite images and models, it remained difficult to obtain clear and quantitative information about the layer base and top heights, the ash density, and its dynamics.

During this event, lidars demonstrated being the only ground based instruments that allow continuous monitoring of the vertical distribution of the volcanic ash. In this paper we present observational results showing the evolution and vertical distribution of the volcanic ash layer over Payerne Switzerland carried out with the MeteoSwiss/EPFL Raman lidar during the whole period of intensive ash emissions.

The MeteoSwiss/EPFL Raman lidar was designed as fully automated instrument for water vapor mixing ratio profiling for the needs of high resolution numerical weather prediction. Recently the lidar was upgraded with a temperature channel employing the pure-rotational Raman method [1, 2, 3]. This upgrade allowed continuous profiling of the tropospheric temperature, relative humidity, and aerosol optical properties.

Aerosol scattering ratio and temperature measurements were retrieved analyzing the Mie and Cabannes elastic scattering and the pure rotational Raman scattering from atmospheric molecules. As a result of the upgrade the lidar provided vertical profiles of aerosol scattering ratio up to

altitude of 10-12 km and with time resolution of 5-30 min. Back trajectories together with the relative humidity profiles were used for identification of the ash layer. Time series of the ash density profiles were calculated as well based on estimation of the ash density from in-situ measurement. The methodology for aerosol scattering ratio measurements analyzing elastic lidar signal and pure rotational spectra is detailed in the following section. Further the lidar instrument description is detailed and finally time series of aerosol scattering ratio and density profiles are presented.

2. Methodology

Pure rotational Raman spectra (PRR) of diatomic molecules such as nitrogen and oxygen consists of approximately regularly spaced spectral lines evenly distributed on either side of the exciting wavelength in Stokes and anti-Stokes branches as shown in Fig.1. The intensity of the lines from the PRR spectra is temperature dependent as defined by the Boltzmann distribution. Therefore analysis of the intensity of individual or set of adjacent lines allows deriving vertical profiles of temperature [3, 4]. Blue and red lines in Fig. 1 represent the envelope of the PRR spectra for two temperatures and the black bold lines represent the spectral passbands of the PRR polychromator for the current setup.

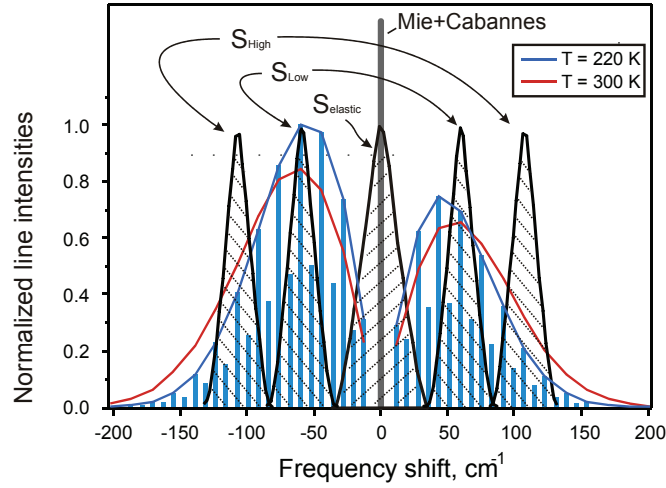


Fig. 1. PRR spectrum of nitrogen calculated at 220 and 300 K.
(The spectral lines of oxygen are omitted for simplicity.)

The ratio of the lidar return signals from low and high portions of the PRR spectra - $S_{Low}(z)$ and $S_{High}(z)$ that are isolated from the spectral passbands indicated in Fig.1 is a function of the atmospheric temperature [3]:

$$R(T(z)) = \frac{S_{Low}(z)}{S_{High}(z)} \approx \exp\left(\frac{\alpha_{\Sigma}}{T(z)} + \beta_{\Sigma}\right). \quad (1)$$

Taking the ratio of the signals cancels the lidar instrument constants and the vertical temperature profile is derived as following [3]:

$$T(z) = \alpha_{\Sigma} / (\ln R(z) - \beta_{\Sigma}), \quad (2)$$

where α_{Σ} and β_{Σ} are calibration constants. In this approach the atmospheric transmission for the signals is neglected since the isolated PRR lines are contained within about 300 cm^{-1} around the laser excitation line. The difference between the detected wavelengths is small to require correction for differential atmospheric attenuation.

The aerosol scattering ratio is measured using the ratio of the elastically scattered light within the Mie and Cabannes lines to the combined PRR signal consisting of all isolated PRR lines. The

passbands of the PRR polychromator for lines with low and high quantum numbers are selected for nearly opposite temperature derivatives of the signals. As a result the summed PRR signal $S_{Sum} = S_{Low} + S_{High}$ decreases with about 3.5% for temperature decrease of 80 K and depends only on the molecular number density and atmospheric transmission, allowing to derive aerosol scattering ratio.

The aerosol scattering ratio is defined as the ratio of total backscatter coefficient including aerosol and molecular contributions $\beta_{tot}(z) = \beta_m(z) + \beta_a(z)$, to the molecular backscatter coefficient $\beta_m(z)$:

$$\mathfrak{R}(z) = \beta_{tot}(z) / \beta_m(z) = 1 + \beta_a(z) / \beta_m(z) \quad (3)$$

and is derived from the ratio of the elastic $S_{Elastic}$ to the PRR signal S_{Sum} :

$$\mathfrak{R}(z) = C S_{Elastic}(z) / S_{Sum}(z) \quad (4)$$

The signal ratio does not depend on system specific constants (i.e. overlap function, transmission, laser power) that are equal for both signals. In this equation the calibration constant C is derived for altitudes with minimum aerosol load (i.e. free atmosphere or below a cloud where a minimum of the scattering ratio could be found).

Ash layer density profiles are obtained from aerosol backscatter coefficient:

$$\rho(z) = K \beta_a(z), \quad (5)$$

where the aerosol backscatter $\beta_a(z) = \mathfrak{R}(z)\beta_m(z)$ is retrieved from lidar measured aerosol scattering ratio and a profile of the molecular backscatter coefficient that is obtained from US standard atmosphere. The constant K in the above equation depends on the ratio of mean particles mass m_a to the aerosol differential backscattering cross-section σ_a^x , both specific for the observed ash layer. Difficult to derive the constant can be obtained by calibration, comparing the lidar measurement of aerosol backscattering coefficient to in-situ density measurement (mass concentration) within the layer.

3. Raman Lidar

The Meteoswiss/EPFL Raman lidar RALMO was build to provide continuous high resolution profiling of water vapor within the troposphere and thus to help improving the data available for initialization of the operational numerical weather prediction models. Daytime measurements of the mixing ratio with vertical range of several kilometers are achieved with narrow field-of-view lidar receiver (0.2 mrad) and narrow spectral band detection (0.3 nm) of ro-vibrational Raman scattering from water vapor and nitrogen. The lidar transmitter employs frequency tripled Nd:YAG Q-switched laser (Continuum 9030) generating short laser pulses (8 ns) with energy of 300 - 400 mJ at 355 nm. The lidar telescope receiver consists of four f/3.33, 30 cm in diameter telescopes that are tightly arranged around a 15x beam expander. The telescopes are coupled by fibers to the water vapor grating polychromator [5].

Long-pass edge filters, installed in front of each fiber prevent systematic errors in water vapor measurements due fluorescence in the fibers excited from the strong elastically scattered light. The cutoff wavelength of the filters (Razor edge of Semrock) is 365.4 nm and the rejection at the laser line is 10^6 . In two of the telescopes the edge filters (REF) are installed at 9° to the telescope axis and reflect Mie, Cabannes, and atmospheric pure rotational Raman spectra to the entrance of multimode fused silica fibers with core diameter of 0.4 mm (see Fig. 2). The light is further transmitted to the entrance of a double stage grating polychromator for temperature and aerosol profiling [6].

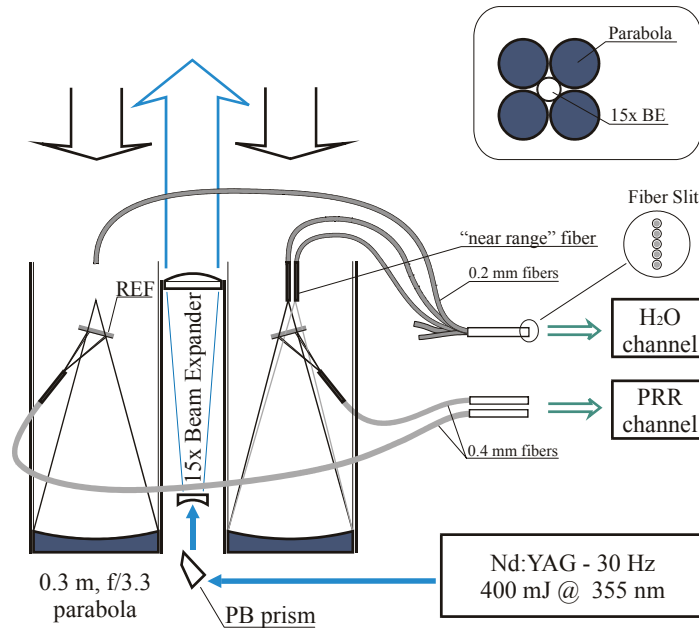


Fig. 2. Optical diagram of the transceiver of RALMO (PB - Pellin Broka prism)

The polychromator (Fig. 3) consists of two identical Litrow configuration stages with 600 gr/mm gratings that are operated at 7th order, and have inverse linear dispersion of ~ 0.53 nm/mm. The stages are set up in a cross-dispersion scheme for better than 10^8 suppression of the elastic light in the PRR channels being important for precise temperature measurements. The elastically scattered light is spectrally isolated by the first stage and is transmitted by two fibers to the designated photomultiplier detector. The four portions of the PRR spectrum, isolated from the first stage, are transmitted by 0.6 mm fibers to the entrance of the second stage to further filter out the residual elastic light. At the exit the PRR lines with the same quantum numbers from Stokes and anti-Stokes branches are recombined in low and high quantum number channels and are transmitted by fibers to the corresponding photomultipliers [7].

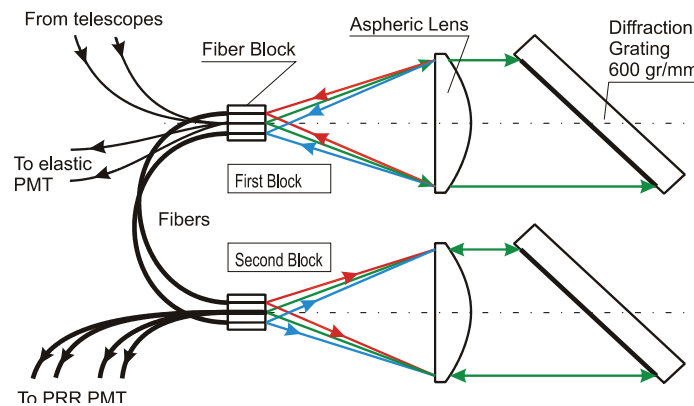


Fig. 3. Optical diagram of the fiber coupled double stage PRR polychromator.

4. Measurements

The volcano ash cloud was detected over Payerne aerological station in the evening of 16 April 2010. An elevated aerosol scattering ratio was detected at an altitude of approximately 6.5 km above ground level at around 21h30 UTC. The aerosols within the layer were originating from the area around the erupting Iceland volcano as proven by the NOAA HYSPLIT model [8]. Moreover the relative humidity within the layer as measured from the lidar was lower than 20 %. This was considered as an indication that the layer is probably not a thin cloud.

Further observations of the evolution of the aerosol layer can be seen on Fig. 4. The figure presents time series of aerosol backscatter ratio defined as $\beta_a(z)/\beta_m(z) = \mathfrak{R}(z) - 1$, (see eq.3) obtained by the lidar signals using eq.4. The time series were obtained with 5 min averaging and fixed vertical resolution of 30 m.

Analyzing the measurement one can see that the ash layer was descending slowly. The aerosol backscatter ratio reached a maximum at 12h UTC on 17 April 2010 at an altitude of about 2.5 km AGL. At the beginning of the next day the layer was detected below 3 km as can be seen from the figure and started to mix with the residual layer.

During the day on 17 April slight mist within the boundary layer lead to high backscatter ratio values from early morning to about midday. In some cases scattered clouds formed at the top of the boundary layer and obstructed the laser beam leading to straight noisy lines as seen on the time series. High altitude clouds formed after midnight on 18 April at altitude of approximately 8.5 km. They are easily distinguished by the aerosol backscatter ratio that is higher than one.

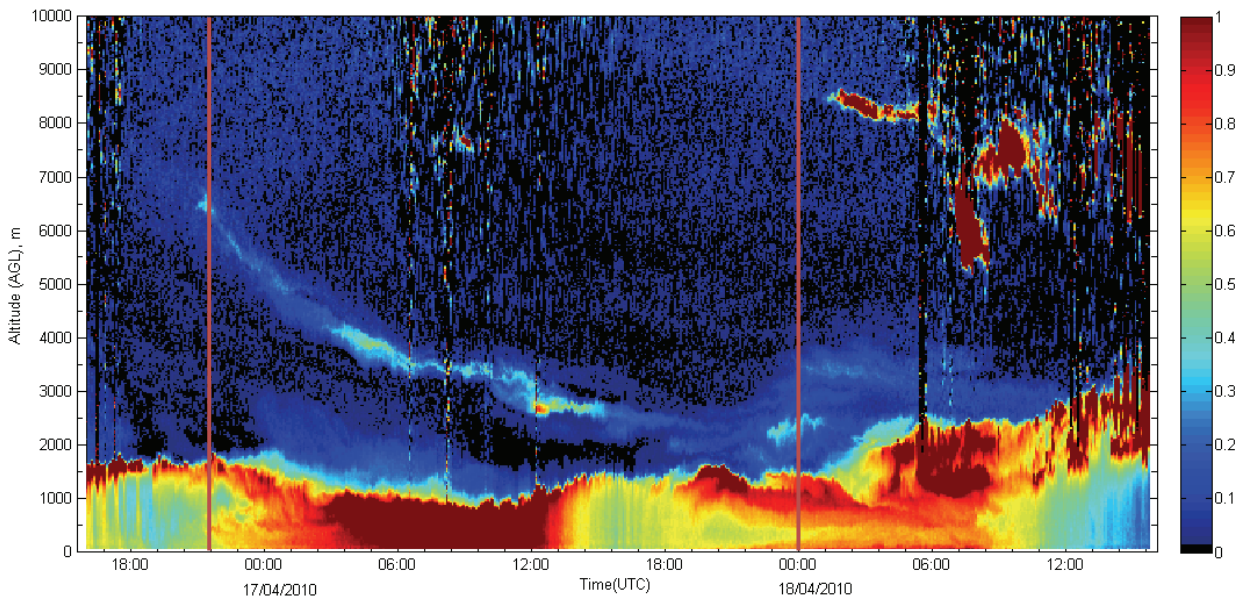


Fig. 4. Time series of aerosol backscatter ratio from 16 April to 18 April 2010 over Payerne.

Confirmation of the origin of the observed aerosol layer is obtained analyzing backward trajectories from the NOAA HYSPLIT model [8]. Two cases are analyzed here with back trajectories presented in Fig. 5; the first case is at 22h UTC on 16/04/2010 when the elevated aerosol layer was for the first time observed at about 6.4 km. The volcanic origin of the layer is confirmed by the back trajectories. The second case is at midnight on 18/04/2010, when two layers with elevated backscatter are observed above the residual layer; the first layer at about 2.2 km, and a second one at about 3.4 km. The back trajectories indicate that the first layer is not originating from the erupting volcano whereas the second layer at 3.4 km is clearly originating from the area of volcanic activity.

Confirmation for the origin of the aerosol layer is obtained as well from the low relative humidity measured by the lidar. The relative humidity profiles were derived from temperature and water vapor mixing ratio profiles obtained with 30 min averaging. Fig. 6 presents the two cases with aerosol backscatter ratio and relative humidity profiles. In either case the relative humidity is relatively low within the ash layer. At 22h on 16 April one can see relative humidity in the range of 30 % at the peak of the backscatter ratio which is observed at about 6.4 km. In the second case, at midnight on 18 April, the relative humidity within the layer at 3.4 km is lower than 20% possibly because of the hygroscopic ashes. The origin of the lower aerosol layer at about 2.2 km however is not clearly related to the volcanic eruption. The relative humidity within the layer is reaching 60 % which could lead to the conclusion that the layer is related to formation of a cloud.

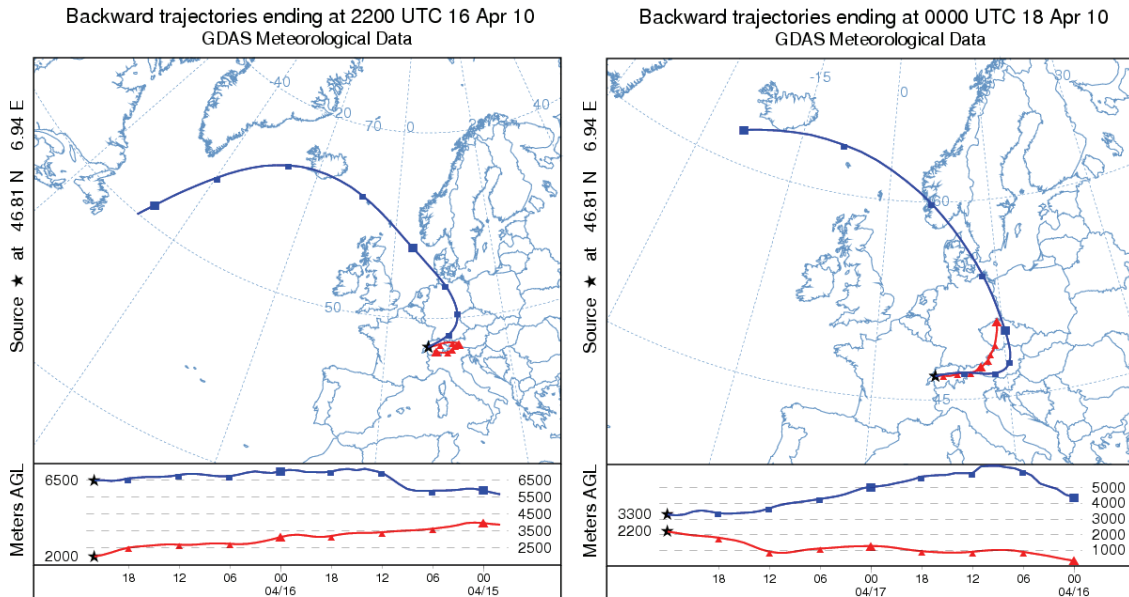


Fig. 5. Backward trajectories from NOAA HYSPLIT model indicating that the origin of atmospheric layers over Payerne on 16/04/2010 at 22h UTC and on 18/04/2010 at 00h UTC is over Iceland.

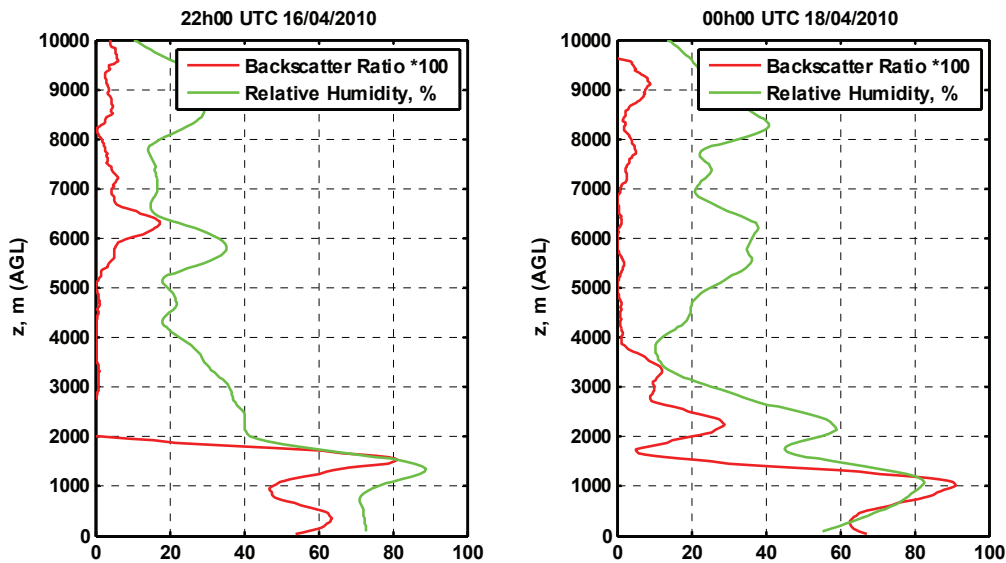


Fig. 6. Vertical profiles of the aerosol backscatter ratio and relative humidity over Payerne as measured from the lidar obtained on 16/04/2010 at 22h00 UTC and on 18/04/2010 at 00h00 UTC.

Finally Fig. 7 presents density profiles estimated from the aerosol backscatter ratio using eq.5 and calibration from preliminary density in-situ measurements from a radiosonde from ETHZ (Technical University at Zurich) [9]. The ash layer is indicated on the plot whereas the layer above ground up to approximately 2 km is identified as the boundary layer.

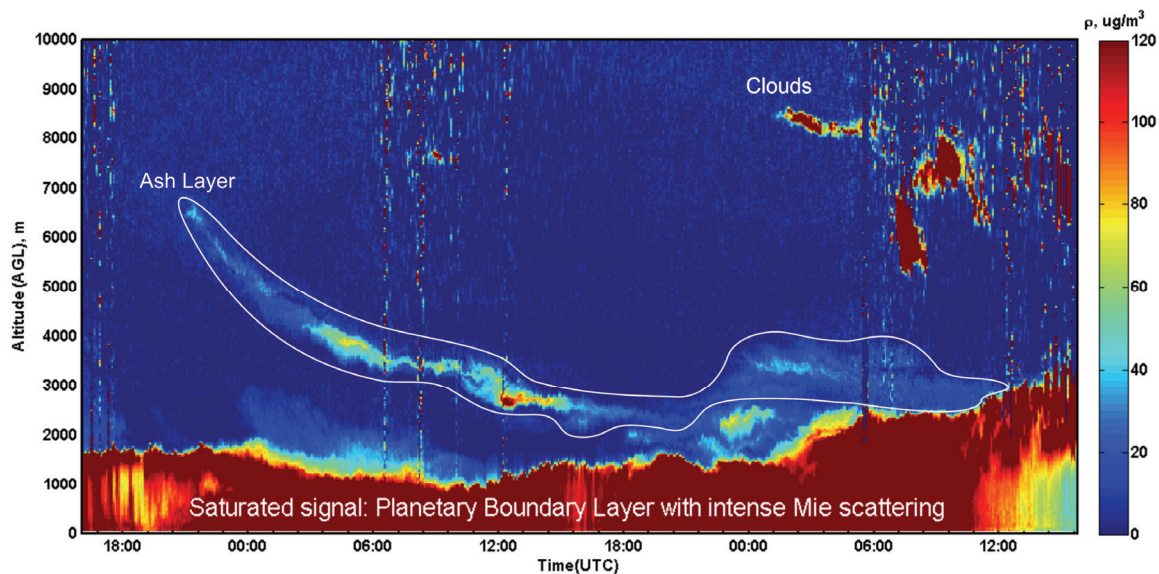


Fig. 7. Density profiles of the volcano ash layer observed over Payerne.

5. Conclusions

In this paper we presented aerosol backscatter ratio measurements with ground based Raman lidar that allowed continuous monitoring of the vertical distribution of the volcanic ash originating from Iceland. Simple calibration of the lidar allowed obtaining density profiles of the ash layer that add valuable information for the vertical extent of the layer and its danger to the air traffic. Simultaneously retrieved relative humidity profiles helped for identification of the aerosols origin but exact identification of the ash layer was based on HYSPLIT back trajectories. Although the valuable for the aviation authorities density profiles were based on preliminary estimations it is clear that lidars with similar capabilities as the Meteoswiss/EPFL Raman lidar could be effectively used for continuous monitoring of ash layers in case of volcano eruptions. Such layers could be quantitatively monitored by lidars provided a single in-situ density measurement is available for initial calibration.

References

1. J. Cooney, "Measurement of atmospheric temperature profiles by Raman backscatter," *J. Appl. Met.* **11** (1972), pp. 108–112.
2. Yu. F. Arshinov, *et al.*, "Atmospheric Temperature Measurements Using Pure Rotational Raman Spectrum and Lidar Calibration," ILRC9, Munich, (1979), pp. 21.
3. Yu. F. Arshinov, *et al.*, "Atmospheric Temperature Measurements Using a Pure Rotational Raman Lidar," *Appl. Opt.* **22**, (1983).
4. G. Vaughan *et al.*, "Atmospheric temperature measurements made by rotational Raman scattering", *Appl. Opt.* **32**, (1993).
5. Dineev T., *et al.*, "Meteorological water vapor Raman lidar – advances", ILRC23, Japan, (2006).
6. A. Ansmann, Yu. Arshinov, S. Bobrovnikov, I. Mattis, I. Serikov, U. Wandinger, "Double grating monochromator for a pure rotational Raman-lidar", *Proceedings of SPIE Vol. 3583*, (1998), pp.491-497.
7. Dineev T., V. Simeonov, *et al.*, "Temperature and aerosol backscatter ratio measurements with the Swiss Raman lidar for meteorological applications", ILRC25, Russia, (2010).
8. Draxler, R.R. and Rolph, G.D., 2010. HYSPLIT (HYbrid Single-Particle Lagrangian Integrated Trajectory) Model access via NOAA ARL READY Website (<http://ready.arl.noaa.gov/HYSPLIT.php>). NOAA Air Resources Laboratory, Silver Spring, MD.
9. Personal communication with Thomas Peter, Swiss Federal Institute of Technology (ETH), Institute for Atmospheric and Climate Science, Universitatstrasse 16, CHN O12.1, CH-8092 Zurich, Switzerland